Brain delivery of fibronectin through bioactive phosphorous dendrimers for Parkinson's disease treatment via cooperative modulation of microglia

Waicong Dai, Mengsi Zhan, Yue Gao, Huxiao Sun, Yu Zou, Regis Laurent, Serge Mignani, Jean Pierre Majoral, Mingwu Shen, Xiangyang Shi

Bioactive Materials 38 (2024) 45–54

Contents lists available at ScienceDirect

Bioactive Materials

journal homepage: www.keaipublishing.com/en/journals/bioactive-materials

Brain delivery of fibronectin through bioactive phosphorous dendrimers for Parkinson's disease treatment via cooperative modulation of microglia

Waicong Dai [a], Mengsi Zhan [a], Yue Gao [a], Huxiao Sun [a], Yu Zou [b,c], Régis Laurent [b,c], Serge Mignani [d], Jean-Pierre Majoral [b,c], Mingwu Shen [a,**], Xiangyang Shi [a,d,*]

[a] State Key Laboratory for Modification of Chemical Fibers and Polymer Materials, Shanghai Engineering Research Center of Nano-Biomaterials and Regenerative Medicine, College of Biological Science and Medical Engineering, Donghua University, Shanghai, 201620, PR China
[b] Laboratoire de Chimie de Coordination du CNRS, 205 Route de Narbonne, CEDEX 4, 31077, Toulouse, France
[c] Université Toulouse, 118 Route de Narbonne, CEDEX 4, 31077, Toulouse, France
[d] CQM-Centro de Química da Madeira, Universidade da Madeira, Campus Universitário da Penteada, 9020-105, Funchal, Portugal

ARTICLE INFO

Keywords:
Phosphorous dendrimers
Fibronectin
Parkinson's disease
Blood brain barrier
Combination therapy

ABSTRACT

Effective treatment of Parkinson's disease (PD), a prevalent central neurodegenerative disorder particularly affecting the elderly population, still remains a huge challenge. We present here a novel nanomedicine formulation based on bioactive hydroxyl-terminated phosphorous dendrimers (termed as AK123) complexed with fibronectin (FN) with anti-inflammatory and antioxidative activities. The created optimized AK123/FN nanocomplexes (NCs) with a size of 223 nm display good colloidal stability in aqueous solution and can be specifically taken up by microglia through FN-mediated targeting. We show that the AK123/FN NCs are able to consume excessive reactive oxygen species, promote microglia M2 polarization and inhibit the nuclear factor-kappa B signaling pathway to downregulate inflammatory factors. With the abundant dendrimer surface hydroxyl terminal groups, the developed NCs are able to cross blood-brain barrier (BBB) to exert targeted therapy of a PD mouse model through the AK123-mediated anti-inflammation for M2 polarization of microglia and FN-mediated antioxidant and anti-inflammatory effects, thus reducing the aggregation of α-synuclein and restoring the contents of dopamine and tyrosine hydroxylase to normal levels *in vivo*. The developed dendrimer/FN NCs combine the advantages of BBB-crossing hydroxyl-terminated bioactive *per se* phosphorus dendrimers and FN, which is expected to be extended for the treatment of different neurodegenerative diseases.

1. Introduction

Neurodegeneration refers to the progressive loss of neuronal structure and function, resulting in cognitive impairment, neuronal death, and imbalanced glial cell activity. An a representative degenerative disease in the central nervous system [1], Parkinson's disease (PD) is characterized by symptoms of resting tremor, bradykinesia, myotonia, kyphosis, postural instability, and accompanied psychiatric manifestations [2]. The primary causes of PD include the degeneration or apoptosis of dopaminergic neurons in the substantia nigra, the misfolding and aggregation of α-synuclein (α-syn), as well as formation of Lewy bodies in the striatum [3,4]. The development of these PD pathologic conditions has been considered to be attributed to the oxidative stress, neuroinflammation, mitochondrial dysfunction, and other related pathological mechanisms [5–8]. Current treatments of PD primarily rely on drugs that modulate dopamine levels, anticholinergics, and glutamate antagonists. Surgical interventions, such as neuronal nuclei destruction and deep brain stimulation, are also employed as alternatives [9]. However, chemotherapy is often limited by the presence of the blood-brain barrier (BBB) and lack of targeted drug delivery systems, and surgical procedures always generate the risk of triggering inflammation and potential brain damage [10,11].

The BBB is a dynamic and highly selective physical barrier in the brain that shields the brain from the influence of toxic substances

Peer review under responsibility of KeAi Communications Co., Ltd.
* Corresponding author. State Key Laboratory for Modification of Chemical Fibers and Polymer Materials, Shanghai Engineering Research Center of Nano-Biomaterials and Regenerative Medicine, College of Biological Science and Medical Engineering, Donghua University, Shanghai, 201620, PR China.
** Corresponding author.
E-mail addresses: mwshen@dhu.edu.cn (M. Shen), xshi@dhu.edu.cn (X. Shi).

https://doi.org/10.1016/j.bioactmat.2024.04.005
Received 28 February 2024; Received in revised form 31 March 2024; Accepted 8 April 2024
Available online 23 April 2024

circulating in the blood and maintains its fundamental stability [12–14]. However, the protective nature of the BBB poses a significant challenge for traditional drugs used in the treatment of brain diseases, as they struggle to reach the site of brain injury [15]. Consequently, achieving desired intracerebral drug concentration often necessitates a high dosing of drugs, which may lead to substantial drug resistance and undesirable toxic side effects [16]. Thus, the development of a drug delivery system capable of penetrating the BBB and targeting brain lesion are crucial for effective treatment of neurodegenerative diseases.

During the progression of PD, the integrity of the BBB becomes compromised [17]. In a recent study, polyethylene glycol-decorated poly(amidoamine) (PAMAM) dendrimers with dense surface hydroxyl groups have been demonstrated to be capable of traversing the compromised BBB and target the activated microglia and inflamed region within the affected area and to exert anti-inflammatory and antioxidant therapeutics [18]. Besides PAMAM dendrimers, phosphorus dendrimers not only exhibit the highly branched, symmetrical structure and uniform molecular weight, but also possess distinctive biological characteristics due to the existence of phosphorus [19]. Phosphorus dendrimers have also emerged as promising carriers, owing to their advantageous attributes such as efficient synthesis, cost-effectiveness, and good biocompatibility, which are promising for applications in neurodegenerative disorders. In earlier studies, Majoral and coworkers demonstrated the effect of phosphorus dendrimers with different generations to inhibit α-syn fibril formation [20,21], suggesting their potential as inhibitors of α-syn aggregation. Therefore, we assume that low-generation phosphorus dendrimers with terminal hydroxyl groups can play their role in permeating the damaged BBB and inhibiting α-syn aggregation for enhanced PD treament.

Fibronectin (FN), a protein composed of two subunits connected by disulfide bonds, is widely present in various tissues, extracellular matrices, body fluids, and blood, and exhibits diverse biological functions [22]. As a major non-collagenase protein in the extracellular matrix, FN plays a pivotal role in facilitating cell surface interactions and participating in essential biological processes, including cell differentiation, growth, and adhesion [23,24]. Notably, FN is known to directly modulate the behavior of macrophages by recognizing and activating integrins *via* the arginine-glycine-aspartic acid (RGD) sequence on its molecular backbone [25]. On the other hand, the microglial membrane surface overexpresses $\alpha_4\beta_1$ integrin [26], in particular in the case of brain injury [27]. Hence, FN may have a good brain inflammation targeting effect due to its RGD motif-containing molecular backbone. Prior studies have shown that pre-adsorption or functionalization of FN on biological scaffolds can effectively reduce the expression of the macrophage inflammatory factor IL-1β [28]. Additionally, FN can significantly inhibit apoptosis of lipopolysaccharide (LPS)-stimulated mesenchymal stem cells-hepatocyte-like cells to improve liver function repair and enhance survival rates of LPS-induced severe combined immunodeficiency *in vivo* [29,30]. The anti-inflammatory and protective effects of FN are likely achieved through the inhibition of the nuclear factor-kappa B (NF-κB) pathway [31]. Furthermore, FN adsorbed on TiO_2 surface was found to induce macrophage polarization towards the M2 phenotype *via* binding with macrophage integrins [32]. Consequently, FN holds a significant potential as a therapeutic protein for treating inflammatory diseases by promoting macrophage polarization and reducing the expression of inflammatory factors. Previous research has also yielded compelling evidence for the anti-inflammatory and antioxidant effects of FN, as well as its ability to transform macrophages from M1

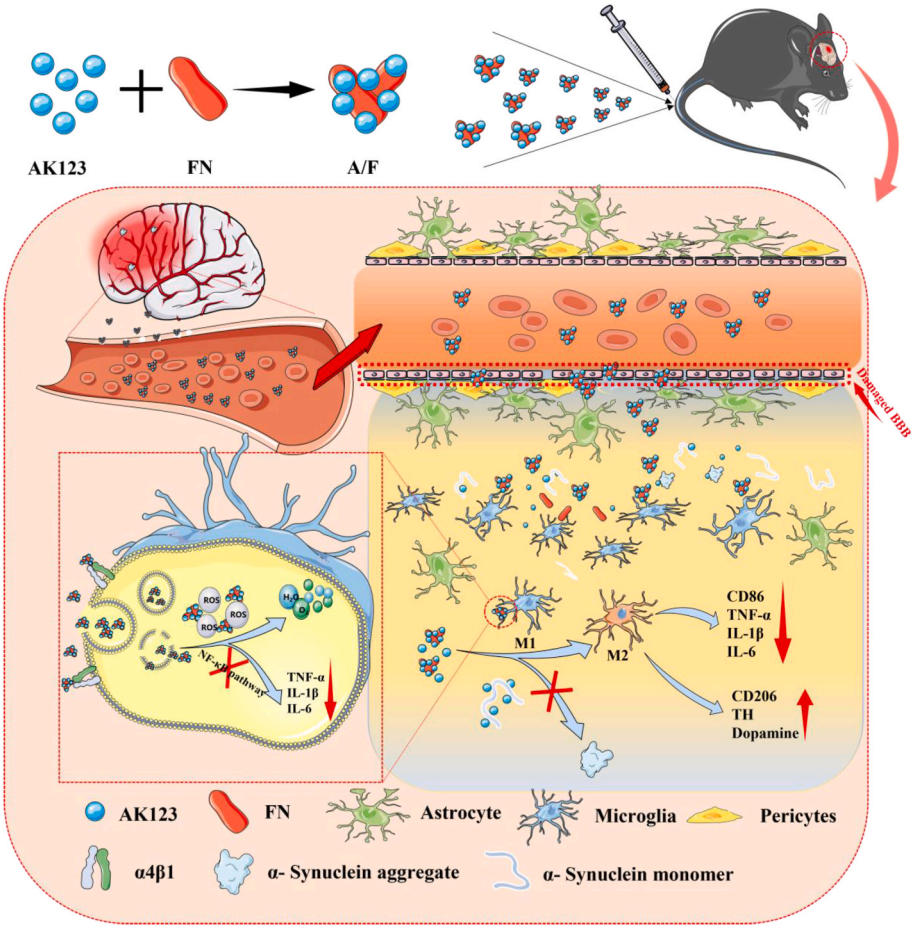

Scheme 1. Schematic illustration of the preparation of AK123/FN NCs for combined treatment of PD *via* M2 microglia polarization, oxidative stress mitigation, inflammatory response suppression and α-syn aggregation inhibition.

phenotype to the M2 one after its effective intracellular delivery to macrophages through a dendrimer-based carrier system [33,34].

In this study, the objective is to investigate the potential of combining a hydroxyl-terminated phosphorous dendrimer (AK123, Fig. S1) with FN to form nanocomplexes (NCs) for PD treatment by targeting microglia and exploiting the anti-inflammatory and antioxidant properties of FN and the intrinsic anti-inflammatory activity of AK123 (Scheme 1). The created AK123/FN NCs were prepared through electrostatic interaction, hydrogen bonding, cation-π and hydrophobic interactions [34]. The size, morphology, and zeta potential of AK123/FN NCs were investigated. Their effects on reactive oxygen species (ROS) scavenging, M2 microglia polarization, and inflammation inhibition were evaluated *in vitro*. The combined anti-inflammatory/antioxidant treatment of a PD mouse model *in vivo* using the AK123/FN NCs was also verified. The prepared AK123/FN NCs exhibit several advantages: 1) the AK123/FN NCs can be easily prepared and are quite stable in aqueous solution with good dispersibility, and the FN complexation can readily improve the water dispersibility of AK123; 2) the terminal hydroxyl groups of the dendrimers confer the AK123/FN NCs to penetrate the damaged BBB for targeted delivery of FN and AK123 to brain PD lesion site through FN-mediated targeting of microglia cells overexpressing integrin $\alpha_4\beta_1$; and 3) the AK123/FN NCs can exert collaborative PD treatments through the combined anti-inflammatory and antioxidant effects for microglia polarization from M1 phenotype to M2 one, inhibition of the NF-κB signaling pathway to reduce the expression of inflammatory factors, and inhibition of the α-syn aggregation, thereby impeding the progression of PD.

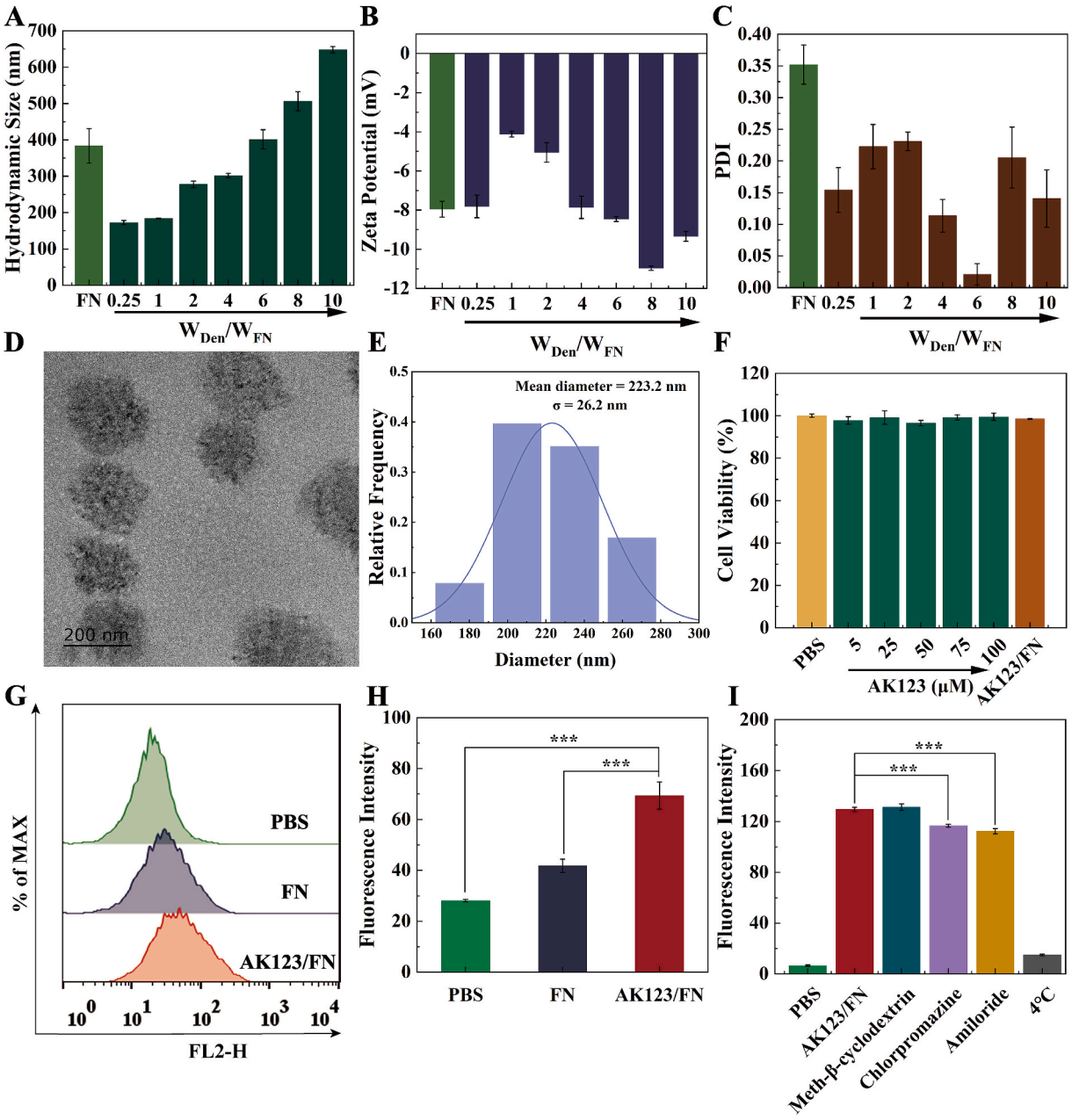

Fig. 1. (A) Hydrodynamic size, (B) zeta potential and (C) PDI of free FN or AK123/FN NCs under different AK123/FN mass ratios (0.25, 1, 2, 4, 6, 8, and 10, respectively). (D) TEM image and (E) size distribution histogram of AK123/FN NCs at an AK123/FN mass ratio of 4. (F) Viability of BV2 cells after treatment with different concentrations of AK123 or AK123/FN ([AK123] = 20.83 μM) for 24 h (n = 6). (G) Flow cytometry histograms and (H) quantification of the fluorescence intensity of BV2 cells after treatment with PBS, free FN, or AK123/FN NCs for 12 h. (I) The cellular uptake pathway evaluation of AK123/FN NCs after BV2 cells were pre-treated with different inhibitors. For A-C, H–I, n = 3 for each sample or measurement, and for H–I, *** for $p < 0.001$.

2. Results and discussion

2.1. Synthesis and characterization of AK123/FN NCs

The hydroxyl-terminated phosphorus dendrimer (AK123, Fig. S1) was synthesized according to the literature [35]. FN was then complexed with AK123 at different AK123/FN mass ratios (0.25, 1, 2, 4, 6, 8 and 10, respectively) to form NCs likely through electrostatic adsorption, hydrogen bonding, cation-π, and hydrophobic interactions. The formed NCs display stable dispersions in aqueous solution (Fig. S2) and were characterized through dynamic light scattering (DLS) and zeta potential measurements (Table S1 and Fig. 1A–C). Free FN shows a hydrodynamic size of 383.8 nm, while the hydrodynamic size of AK123/FN NCs increases with the increase of the AK123/FN mass ratio. It is noticed that the hydrodynamic size of AK123/FN NCs is smaller than that of free FN at the AK123/FN mass ratio lower than 6, suggesting the strong compression ability of the dendrimers to form relatively compacted NCs. Further increase of the AK123/FN mass ratio seems to compromise the compacted structure of the NCs with an improved tendency of aggregation. It is interesting to note that all NCs formed at different mass ratios display negative surface potentials, presumably owing to the fact that the negative surface potential of FN does not change after being complexed with AK123. Furthermore, by centrifuging the NC solution to collect the supernatant for FN concentration quantification using the BCA assay kit, we were able to calculate the encapsulation efficiency (EE) and loading content (LC) of FN in the formed NCs (Table S2). At an AK123/FN mass ratio of 4, the formed NCs showcase a relatively small hydrodynamic size (301.5 ± 6.2 nm) and polydispersity index (PDI, 0.10 ± 0.08), and the EE and LC of FN can be achieved to be 85.2 % and 16.7 %, respectively. Hence, the NCs formed at an AK123/FN mass ratio of 4 was selected for further studies.

Transmission electron microscopy (TEM) was employed to observe the size and morphology of the AK123/FN NCs. As shown in Fig. 1D and E, the AK123/FN NCs display a uniform spherical morphology with a mean particle size of 223.2 ± 26.2 nm. Additionally, sodium dodecyl sulfate-polyacrylamide gel electrophoresis (SDS-PAGE) assay was utilized to characterize the NCs (Fig. S3). It is clear that the AK123/FN NCs show the similar protein bands to FN, further demonstrating the successful loading of FN by the AK123 dendrimers. We also tested the colloidal stability of the AK123/FN NCs through DLS analysis of their hydrodynamic size after they were dispersed in water, phosphate buffered saline (PBS) and cell culture medium for a time period of one week (Fig. S4). Apparently, the NCs display no significant hydrodynamic size changes, indicating their desired colloidal stability. For comparison, we also prepared AK123/bovine serum albumin (BSA) NCs under the AK123/BSA mass ratio at 4: 1. In this case, the EE and LC of BSA can be achieved to be 70.8 % and 15.0 % (Table S3), respectively, and the NCs display a hydrodynamic size of 285.0 nm and a surface potential of −19.3 mV (Table S4), quite comparable to the AK123/FN NCs.

To validate the structural integrity and functional preservation of FN, circular dichroism (CD) was introduced to analyze the secondary structural changes of FN after complexation. As depicted in Fig. S5, the CD spectra of free FN and NCs exhibit remarkable similarity, indicating that the secondary structure of FN can be maintained after its complexation with AK123. This crucial evidence reinforces the potential of NCs as an effective delivery vehicle that can not only promise to efficiently deliver FN but also retain the biological activity of FN.

Furthermore, efficient release of FN from NCs is crucial to exert its biological functions within cells. To validate the intracellular release mechanism of AK123/FN after cellular uptake, we dispersed AK123/FN NCs in phosphate buffer solutions of different pHs and monitored the changes in their hydrodynamic size using DLS (Fig. S6). The results reveal that the uniform size distribution of AK123/FN NCs is disrupted at a low pH condition, as manifested by the appearance of two peaks in the hydrodynamic size distribution of the AK123/FN NCs at pH 6.5, which is different from that at pH 7.4. This implies that the acidic environment within the cells can promote the disruption of the NCs, thereby facilitating the release FN and AK123 to perform their respective functions after celluar uptake.

2.2. Cytotoxicity and cellular uptake assays

The cytotoxicity of AK123/FN NCs was examined by Cell Counting Kit-8 (CCK-8) assay of the viability of BV2 cells (a mouse microglia cell line). As illustrated in Fig. 1F, under the AK123 concentration up to 100 μM for free dendrimers, the cell viability still remains above 95 %. Additionally, BV2 cells treated with the AK123/FN NCs with an AK123/FN mass ratio of 4 also display non-compromised cell viability, thus proving the good cytocompatibility of AK123/FN NCs. To further evaluate the biosafety of the NCs, we assessed their potential immunogenicity through dendritic cells (DCs) maturation assays. The expression levels of the maturation markers CD80 and CD86 on DCs after treatment with different materials were detected using flow cytometry. As shown in Figs. S7A–C, compared to the PBS group, no significant difference in the expression levels of CD80 and CD86 can be seen in various treatment groups. Additionally, the secretion levels of the pro-inflammatory cytokines TNF-α and IL-6 in DCs after different treatments also do not change significantly as compared with the PBS treatment, suggesting that the formed NCs do not induce dendritic cell maturation (Figs. S7D–E). Taken together, the developed NCs possess favorable biocompatibility and non-immunogenicity.

Subsequently, FN was labeled with Cy5.5 dye for cellular uptake assays. The FN-Cy5.5 conjugate was characterized by fluorescence spectrum (Fig. S8A) to show the similar fluorescence emission feature to free Cy5.5 dye. By comparison with the standard curve of the free Cy5.5 fluorescence emission at 697 nm versus concentration, the number of Cy5.5 moieties conjugated to each FN molecule was determined to be 3.8 (Fig. S8B). Next, the cellular uptake efficiency of AK123/FN NCs in BV2 cells was determined by flow cytometry assay of the red fluorescence signals after treatment with free FN-Cy5.5 or AK123/FN-Cy5.5 NCs. Compared to the PBS group, BV2 cells treated with free FN-Cy5.5 exhibit low red fluorescence intensity, indicating a slight phagocytosis of free FN by BV2 cells. Notably, a significant increase in red fluorescence can be observed for BV2 cells treated with the AK123/FN NCs, much higher than the PBS and free FN-Cy5.5 groups (Fig. 1G–H, $p < 0.001$). Moreover, the AK123/FN NCs show a time-dependent uptake by BV2 cells as the red fluorescence intensity of cells gradually increases over time (Fig. S9). These findings provide strong evidence for the excellent intracellular protein delivery ability of AK123/FN NCs.

Furthermore, confocal laser scanning microscopy (CLSM) was employed to investigate the intracellular localization of FN in BV2 cells (Fig. S10). In comparison to the PBS group, BV2 cells treated with free FN-Cy5.5 exhibit weak red fluorescence signals, whereas those treated with the AK123/FN NCs display a substantially increased red fluorescence intensity in the cytoplasm. This observation is consistent with the results obtained from flow cytometry assays, further confirming the efficient intracellular FN delivery capacity of the AK123/FN NCs.

To explore the possible phagocytic pathway of BV2 cells after treated with the AK123/FN NCs, different intracellular endocytosis inhibitors were selected to pre-treat the BV2 cells, followed by measuring the fluorescence intensity of the cells treated with the AK123/FN-Cy5.5 NCs through flow cytometry. As depicted in Fig. 1I, cells treated with chlorpromazine (inhibitor of clathrin-mediated endocytosis) and amiloride (inhibitor of macropinocytosis) exhibit significantly lower red fluorescence intensity than other groups ($p < 0.001$), suggesting that the AK123/FN NCs are taken up by BV2 cells *via* clathrin-dependent and micropinocytosis-mediated pathways. Further, to confirm the role of RGD sequence on the FN in targeting BV2 cells, we pre-treated the cells with RGD peptide and subsequently evaluated the fluorescence intensity of cells *via* flow cytometry (Fig. S11). Apparently, the cellular uptake of NCs significantly decreases after pre-blocking with RGD peptide, suggesting that the FN complexed in the NCs renders them with targeting

specificity to microglia with $\alpha_4\beta_1$ integrin overexpression ($p < 0.001$).

2.3. In vitro anti-inflammatory and antioxidant activity assays

In PD, neuronal damage is primarily caused by the interplay of two major mechanisms of inflammatory response and oxidative stress [36]. We next investigated the anti-inflammatory and antioxidant effects of the AK123/FN NCs *in vitro*. Microglia, immune cells in the central nervous system, play a crucial role and can be categorized into both M1 and M2 phenotypes [37]. The M1-type microglia exhibit pro-inflammatory and neurotoxic effects, while the M2 type ones demonstrate anti-inflammatory and neuroprotective properties [38,39]. To explore the impact of the AK123/FN NCs on the phenotypic polarization of BV2 cells, the cells were first activated by LPS to be predominantly present as M1 type and subsequently treated with FN, AK123, AK123/FN NCs, or AK123/BSA NCs for 24 h. The expression levels of cluster of differentiation 206 (CD206, M2-type marker) and CD86 (M1-type marker) in BV2 cells were analyzed by flow cytometry. As shown in Fig. 2A–D, the CD86 expression levels of BV2 cells treated with LPS alone exhibit a notable increase, confirming the activation of BV2 cells by LPS to be mostly in M1 phenotype. However, when BV2 cells were treated with the AK123/FN NCs, a significant downregulation of CD86, along with a remarkable upregulation of CD206 can be seen, suggesting the effective repolarization of M1 type BV2 cells to M2 type ones. The repolarization of BV2 cells can be further quantitatively proofed through the ratio of CD206/CD86 (Fig. 2D), where the highest ratio of CD206/CD86 can be achieved in the group of AK123/FN NCs among all groups ($p < 0.001$). Notably, free FN does not seem to have such an immune modulation due to the limited FN intracellular delivery, while both free AK123 and AK123/BSA NCs display moderate M2 polarization potential of BV2 cells, presumably owing to the intrinsic anti-inflammatory activity of the phosphorous dendrimers [40]. Hence, due to the combinational anti-inflammation effect of both AK123 and FN for the NCs with improved FN intracellular delivery efficiency, BV2 cells treated with the AK123/FN NCs display the most significant BV2 M2 polarization efficacy among all materials investigated.

To examine the antioxidant activity of the developed NCs, we used an ROS fluorescence probe (2, 7-dichlorofluorescin diacetate) to evaluate the ROS scavenging effect in BV2 cells (Fig. 2E). In comparison with the LPS positive control group, the ROS-derived fluorescence in BV2 cells treated with the AK123/FN NCs significantly reduces. The quantitative results reveal that the group of AK123/FN NCs exhibits the lowest ROS-associated fluorescence intensity among all groups except for the negative PBS control group (Fig. S12, $p < 0.01$), indicating the excellent antioxidant activity of AK123/FN NCs owing to the combined effects of anti-inflammation activity of AK123 and enhanced intracellularly delivered FN. Free FN displays moderate antioxidant activity due to its limited intracellular delivery, while free AK123 and AK123/BSA NCs have the same moderate antioxidant activity likely due to the cooperative anti-inflammation activity of AK123 to polarize the BV2 cells to M2 phenotype.

Then, the expression of inflammatory cytokines in cell culture medium was measured through enzyme-linked immunosorbent assay (ELISA). As shown in Fig. 2F–H, cells treated with free AK123 or free FN display downregulated pro-inflammatory factors including IL-6, IL-1β, and TNF-α, which could be attributed to the ability of AK123 and FN to promote microglia polarization to anti-inflammatory M2 type. Moreover, the lowest level of inflammatory factors can be achieved in the group of AK123/FN NCs among all groups, indicating the excellent anti-inflammatory activity of the NCs. This could be due to the fact that the AK123/FN NCs have improved intracellular delivery efficiency, greatly exerting the anti-inflammatory and antioxidant functions of both AK123 and FN to inhibit the inflammatory response.

Previous study has confirmed that FN delivered by PAMAM dendrimer can achieve anti-inflammatory effects by inhibiting the NF-κB signaling pathway [33]. Western blot assay was next applied to

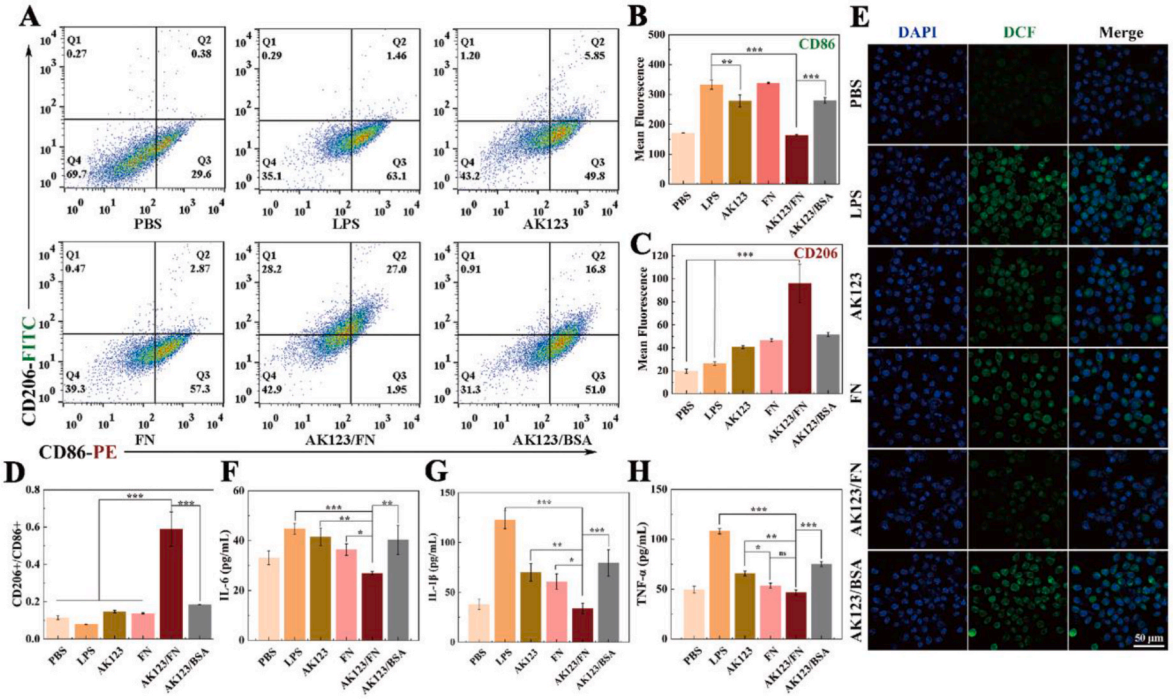

Fig. 2. (A) Flow cytometry analysis of the expression levels of CD86 and CD206 in LPS-activated BV2 cells treated with AK123, free FN, AK123/FN or AK123/BSA. (B, C) Mean fluorescence intensity of (B) CD86 and (C) CD206 expression in BV2 cells obtained from (A). (D) Ratio of CD206/CD86 and (E) CLSM images of ROS in LPS-activated BV2 cells after incubated with FN, AK123, AK123/FN or AK123/BSA for 24 h. ELISA analysis of (F) IL-6, (G) IL-1β and (H) TNF-α expression in LPS-activated BV2 cells treated with FN, AK123, AK123/FN or AK123/BSA for 24 h. For A-G, LPS and PBS were used as positive and negative control, respectively, and the [FN] was 20 μg/mL ($n = 3$ for each group or measurement). In B-D and F-G, ns for no significance, * for $p < 0.05$, ** for $p < 0.01$, and *** for $p < 0.001$, respectively.

investigate the effect of AK123/FN NCs on the NF-κB signaling pathway regulation. As shown in Fig. S13, the expression level of NF-κB after treated with LPS is significantly higher in the cell nucleus and significantly lower in the cytoplasm than that of cells treated with PBS. When BV2cells were treated with AK123 and free FN alone, the NF-κB expression level shows a slight decrease in the cell nucleus and a slight increase in the cytoplasm. It is noticed that in the group of AK123/FN NCs, the NF-κB expression in the nucleus significantly reduces, while remarkably increases in the cytoplasm, almost close to that of cells in the PBS control group. This indicates that the AK123/FN NCs could inhibit the translocation of NF-κB protein from the cytoplasm to the nucleus to downregulate the expression of pro-inflammatory factors.

2.4. *In vivo* biodistribution and pharmacokinetics

An *in vitro* BBB transwell system was firstly established to assess the ability of AK123/FN NCs to cross the BBB (Fig. S14A). The bEnd.3 cells were cultured in the upper chamber until the transendothelial electrical resistance (TEER) reached 200–300 Ω cm^2 to mimic the BBB endothelial monolayer, while BV2 cells were seeded in the lower chamber, representing the brain parenchyma. Fresh culture medium containing different materials (PBS, FN-Cy5.5, or AK123/FN-Cy5.5, [FN] = 20 μg/mL) was respectively introduced into the upper chamber and cells were incubated for 6 h. TEER measurements confirm that the incubation of various materials does not affect the integrity of the bEnd.3 monolayer (Fig. S14B). Subsequently, the BBB permeability was evaluated by monitoring the fluorescence intensity of cells (Figs. S14C–E). The AK123/FN-Cy5.5 group exhibits a relatively lower fluorescence intensity in bEnd.3 cells in the upper chamber than the FN-Cy5.5 group. In contrast, more significant fluorescence can be observed in BV2 cells in the lower chamber with AK123/FN-Cy5.5 treatment than with FN-Cy5.5 treatment ($p < 0.001$). Quantitative data reveal that the BBB penetration efficiency of AK123/FN-Cy5.5 (25.9 %) is 1.8 times higher than that of FN-Cy5.5 ($p < 0.001$, Fig. S14F), indicating that the AK123/FN NCs possess an enhanced ability to cross the *in-vitro* BBB model, and the hydroxylated AK123 enables effective brain delivery of FN (see below).

We next conducted *in vivo* fluorescence imaging to verify the ability of the AK123/FN NCs to penetrate the damaged BBB in a mouse PD model. Before that, a hemolysis experiment was carried out to evaluate the hemocompatibility of the AK123/FN NCs (Fig. S15). Clearly, the hemolysis rates of the mouse red blood cells treated with the NCs at different dendrimer concentrations up to 100 μM are all below 2 %, suggesting the great hemocompatibility of the developed AK123/FN NCs.

Afterwards, the PD mice were intravenously injected with AK123/FN-Cy5.5 NCs or FN-Cy5.5, and *in vivo* imaging was carried out at different time points postinjection (Fig. 3A). Mice in the AK123/FN-Cy5.5 group exhibit evident red fluorescence signals in the brain region, and the fluorescence intensity gradually increases, reaching its peak at 4 h, and then begin to decrease at 6 h postinjection (Fig. S16). In contrast, only slight fluorescence signals can be seen in the mouse brain in the FN-Cy5.5 group. This suggests that the AK123/FN-Cy5.5 NCs could successfully penetrate the BBB to accumulate at the brain region over time, thanks to the hydroxyl groups of the AK123 dendrimers. Ex-

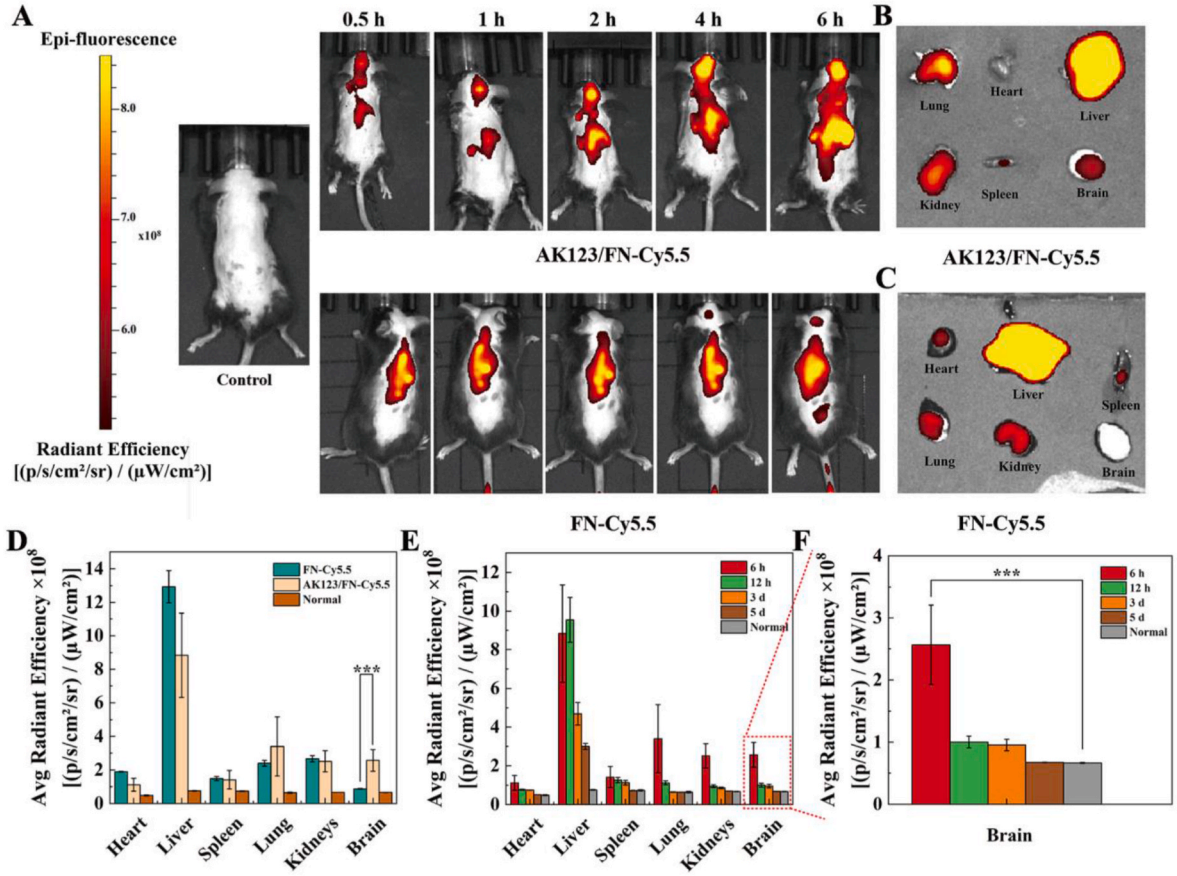

Fig. 3. (A) Fluorescence imaging of live mice at 0.5, 1, 2, 4, and 6 h post tail vein injection of AK123/FN-Cy5.5 NCs and FN-Cy5.5, respectively. *Ex-vivo* fluorescence imaging of main organs including heart, liver, spleen, lung, kidneys, and brain of mice at 6 h postinjection of (B) AK123/FN-Cy5.5 NCs or (C) FN-Cy5.5. (D) Average radiant efficiency of heart, liver, spleen, lung, kidneys, and brain of mice at 6 h postinjection of FN-Cy5.5 and AK123/FN-Cy5.5 NCs, respectively. Biodistribution of AK123/FN NCs in (E) main organs and (F) brain at 6 h, 12 h, 3 days and 5 days postinjection as determined by fluorescence imaging. For D-F, n = 3 for each group or measurement. In D and F, *** for $p < 0.001$.

vivo fluorescence imaging of the extracted organs including the heart, liver, spleen, lung, kidney and brain at 6 h postinjection was also performed. As observed in Fig. 3B–D, a more prominent red fluorescence can be observed in the mouse brain in the AK123/FN-Cy5.5 group than in the FN-Cy5.5 group ($p < 0.001$), in good consistence with the *in vivo* imaging results. Furthermore, significant red fluorescence signals in the liver, lung and kidney can be seen in both groups, suggesting that the majority of AK123/FN-Cy5.5 NCs and FN-Cy5.5 can be accumulated and cleared in these reticuloendothelial system (RES) organs. An extended tissue biodistribution of the AK123/FN NCs in mice was further studied through *in-vivo* fluorescence imaging of the major organs (Fig. 3E and F). The mice treated with the AK123/FN NCs show significantly high fluorescence intensity in the brain at 6 h postinjection than at 5 days postinjection ($p < 0.001$), which is close to the control mice treated with PBS (normal group). It can be observed that except for the liver site, the fluorescence signals of AK123/Cy5.5-FN NCs in the heart, spleen, kidney, and brain is almost indistinguishable from those of normal mice on day 5. Along with peak fluorescence intensity in the liver at 12 h postinjection and gradual decrease of the fluorescence intensity, these results suggest that the developed AK123/FN NCs can cross the damaged BBB and be slowly metabolized with the time through RES organs. Furthermore, pharmacokinetics data show that the FN concentration in the blood decreases for both free FN and AK123/FN NCs within 24 h postinjection, and the AK123/FN NCs exhibit a longer half-decay time (1.137 h) than free FN (0.976 h) *in vivo* (Fig. S17).

2.5. Combined treatment of PD in a mouse model

The PD mouse model establishment, treatment, behavioral training and behavioral testing procedure are shown in Fig. 4A. Firstly, the healthy mice and PD mice were divided into five groups: (1) healthy group (Normal); (2) PD mice injected with normal saline (PD); (3) PD mice injected with free FN group (PD + FN); (4) PD mice injected with AK123/BSA NCs (PD + A/B); and (5) PD mice injected with AK123/FN NCs (PD + A/F). As shown in Fig. 4B, PD mice treated with AK123/FN NCs can persist on the rotary stick for a long time about 142 s in the rotary test, quite similar to the normal mice. For the grip test (Fig. 4C), the grip strength of mice in the AK123/FN group can recover to the best level among all treatment groups except the negative PBS control group ($p < 0.001$), similar to that of normal mice. In addition, in tail suspension test (Fig. 4D) and forced swimming test (Fig. 4E), the immobility time and floating immobility time of mice after treated with the AK123/FN NCs are much shorter than those of PD group, and are close to the level of normal group. From the Videos S1 and S2, it can be observed that in the early stages of the tail suspension and forced swimming experiments, all mice start struggling when faced with extreme conditions. With the time progressing, the PD mice tend to give up struggling earlier, while the PD mice treated with the AK123/FN NCs remain

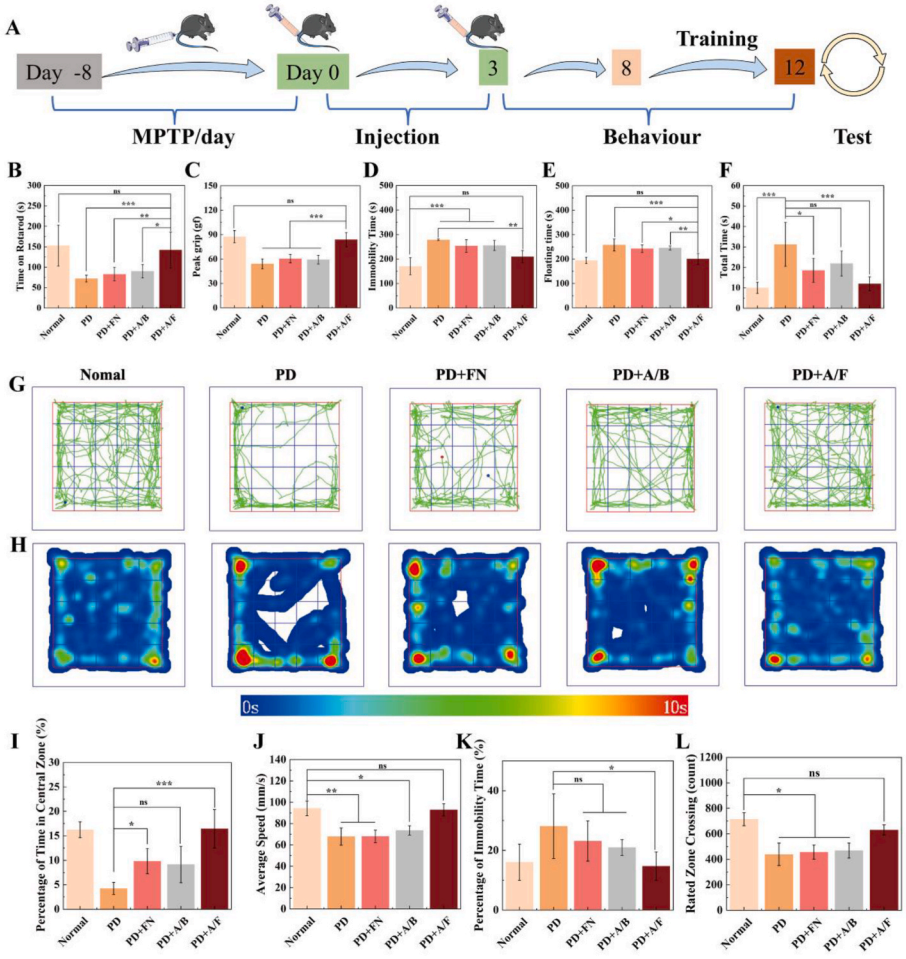

Fig. 4. (A) Schematic diagram of the treatment and test schedule of PD mice. (B) Time on rotarod in rotarod test, (C) the peak grip in grip test, (D) the immobility time in tail suspension test, (E) floating time in forced swimming test and (F) total time in pole test of mice after different treatments. (G) Representative paths of mice from different groups and (H) temporal heat map, (I) percentage of time in central zone, (J) average speed, (K) percentage of immobility time, and (L) rated zone crossing in the open field test of mice in different groups. For B–F and I-L, n = 6 for each group or measurement, ns for no significance, * for $p < 0.05$, ** for $p < 0.01$, *** for $p < 0.001$, respectively.

sustained struggling and a desire to escape in both the tail suspension and forced swimming tests, similar to the behavior of the normal group. Meanwhile, PD mice treated with the AK123/FN NCs spend the shortest time in the pole test among all treatment groups except the normal mice treated with PBS (Fig. 4F, $p < 0.001$). These results indicate that the treatment of the AK123/FN NCs can greatly improve the behavioral ability of MPTP-induced PD mice to vastly recover the level of fatigue resistance and grip strength, as well as exhibit strong desire to struggle and survive in the face of a desperate environment.

In the open field test (Fig. 4G and H), it is noticeable that PD mice tend to stay in the corners and edges of the open field. In contrast, the PD mice after AK123/FN treatment are capable of exploring more towards the center of the open field, similar to that of the normal group. In Video S3, we can observe the aforementioned results more directly. The central region exploration time of PD mice after AK123/FN treatment significantly extends and recovers to a level close to that of the normal group (Fig. 4I). In addition, the average speed, the immobility time and rated zone crossing of PD mice after treatment with the AK123/FN are all close to those of the normal group (Fig. 4J-L), suggesting that the symptoms of PD are significantly alleviated and successfully restored to the normal levels. Based on the above results, we can safely conclude that the AK123/FN treatment is a powerful strategy to tackle PD to improve the behaviors of mice with mental depression.

Supplementary video related to this article can be found at https://doi.org/10.1016/j.bioactmat.2024.04.005

To further validate the *in vivo* therapeutic efficacy of AK123/FN NCs on PD mice, the immunohistochemistry and immunofluorescence staining of brain were performed. As shown in Fig. 5A, the cells in the hippocampal region are closely connected and orderly arranged in the normal group, while for the PD group, the cells in the hippocampal region show disordered arrangement and the loss of neurons. Compared with the PD group, the hippocampal cells of the mice treated with AK-123/BSA or free FN alone can be recovered to some extent, however there are still some deficiencies when compared with the normal group. In the group of AK123/FN NCs, the hippocampal cells of the mice are orderly arranged and return to normal conditions, demonstrating the effective therapeutic effect of AK123/FN NCs. This indicates that the brain damage of PD mice can be alleviated after treatment with the AK123/FN NCs. Meanwhile, Nissl staining was used to analyze the state of neurons in the brain striatum. Compared with the normal group, the PD group shows a large reduction of Nissl bodies. This situation can be slightly improved after the treatment of AK123/BSA or free FN, while the AK123/FN treatment leads to significantly increased Nissl bodies in the striatum, which is close to normal group. These results might be due to the enhanced intracellular delivery of AK23/FN NCs, thus exerting improved anti-inflammatory and antioxidant effect of both materials to

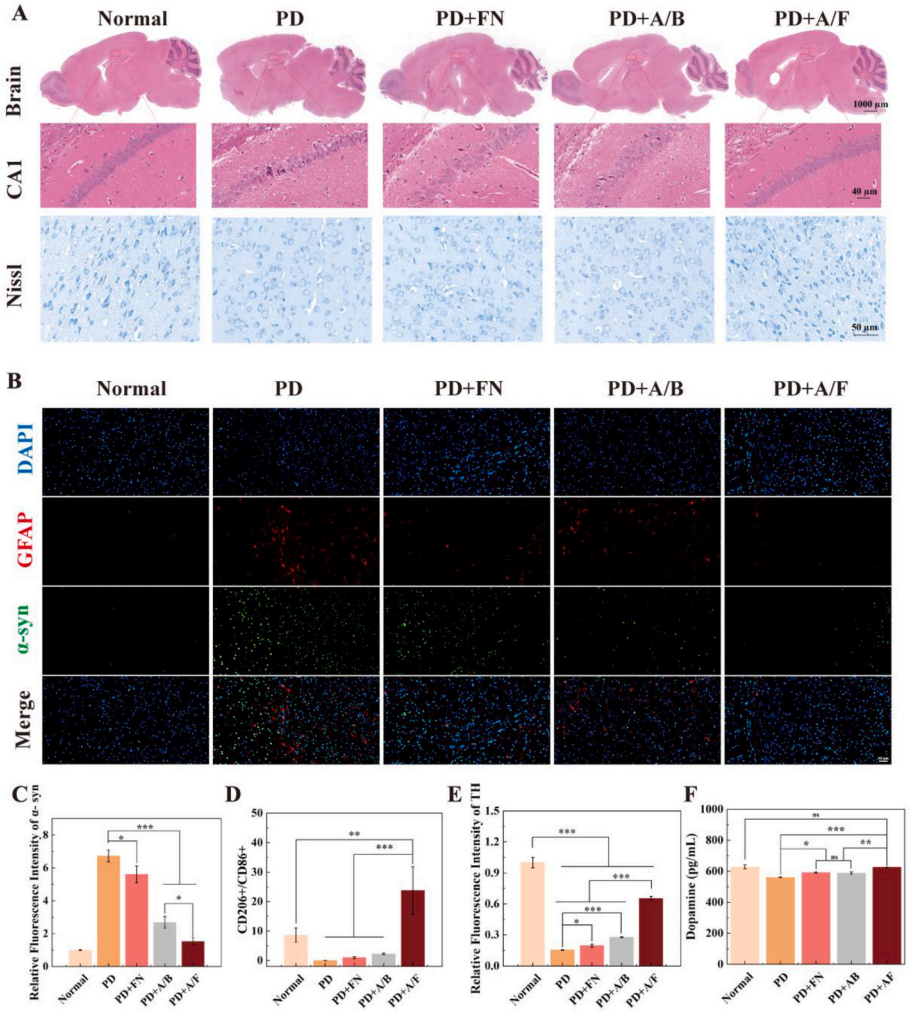

Fig. 5. (A) H&E staining images of brain and CA1 region of the hippocampus, and nissl staining of neurons. (B) Immunofluorescence staining of GFAP and α-syn of the striatum in different groups of mice. (C) Relative fluorescence intensity of α-syn. (D) The ratio of CD206+/CD86+. (E) Relative fluorescence intensity of TH in mouse brain after different treatments. (F) Relative levels of dopamine collected from mouse brains in different groups. For C–F, $n = 3$ for each group or measurement, ns for no significance, * for $p < 0.05$, ** for $p < 0.01$, *** for $p < 0.001$, respectively.

greatly reinforce the treatment of PD through neuron protection from damage.

Additionally, the brain of mice in each group was sliced and stained with glial fibrillary acidic protein (GFAP)/α-syn antibodies for immunofluorescence analysis (Fig. 5B). In contrast to the PD group showing significant upregulation of α-syn and GFAP (a marker of astrocyte activation), the treatment of AK123/FN NCs leads to significant downregulation of α-syn and GFAP, which is quite similar to the normal group. Quantitative analysis of the expression of α-syn reveals that the treatment of AK123/FN NCs leads to the lowest α-syn expression among all groups except the normal group (Fig. 5C, $p < 0.05$), which may be due to the fact that AK123 can inhibit the accumulation of α-syn in the brain so as to prevent the deterioration of PD [20,21].

To examine the polarization state of BV2 cells in the brain after different treatments, immunofluorescence staining of CD206 and CD86 of the striatum was performed (Fig. S18). BV2 cells in the brain of PD group displays decreased expression of M2 marker CD206 (green fluorescence) and simultaneous increased expression of M1 marker CD86 (red fluorescence). After treatment with the AK123/FN NCs, a significant upregulation of CD206 expression (green) and downregulation of CD86 expression (red) can be seen in the mouse brain. Further quantitative of the green/red fluorescence intensity ratio reveals that the treatment of AK123/FN NCs achieves the highest ratio of CD206/CD86 among all groups ($p < 0.01$), indicating that the developed AK123/FN NCs could promote the transformation of microglia from M1 phenotype to M2 one in the brain of PD mice (Fig. 5D).

Furthermore, we also analyzed the expression levels of ionized calcium binding adaptor molecule-1 (IBA-1, a marker of microglia inflammation in the mouse brain) and TH (a marker indicating the capability of dopamine synthesis) in the mouse striatum through immunofluorescence staining after various treatments (Fig. S19). Clearly, the treatment of AK123/FN NCs leads to apparent downregulation of IBA-1 and upregulation of TH, which can also be proofed through quantitative assay of the relative fluorescence intensity (Figure S20 and Fig. 5E, $p < 0.001$ among all groups except the normal group treated with PBS). This suggests that the treatment of AK123/FN NCs leads to apparent reduction of microglia inflammation and improved dopamine synthesis, thus alleviating the PD symptoms. In order to further verify the function and therapeutic effect of AK123/FN NCs, the brain samples of mice from different groups were collected to measure the dopamine levels by ELISA (Fig. 5F). As can be seen, in contrast to the positive control group of PD mice with low dopamine level, the treatment of AK123/FN NCs leads to a significantly increased dopamine level in the brain ($p < 0.01$ compared to other groups except the normal group), which is quite close to the normal group. These results suggest that the effective therapeutic effect of AK123/FN NCs on PD treatment can be realized through enhanced anti-inflammatory and antioxidant therapy of the mouse brain, thereby protecting the brain from inflammation and damage.

2.6. *In vivo* biosafety investigation

The biosafety of the AK123/FN NCs was lastly evaluated by hematoxylin-eosin (H&E) staining of the major organ slices of PD mice *in vivo* after different treatments for 48 h. As shown in Fig. S21, all treatment materials do not seem to significantly affect the histomorphology of major organs include heart, liver, spleen, lung and kidney of mice, similar to the PBS control group. To verify the long-term biosafety of NCs, the major organs (heart, liver, spleen, lung, kidney, and brain) of the mice after NCs treatment for 7 days were collected for H&E staining analysis (Fig. S22). The results show that the major organs of the mice are not impacted, demonstrating the good long-term biosafety of NCs. Along with the proven good hemocompatibiliy of the NCs through hemolysis assay (Fig. S15) and the pharmacokinetics and the biodistribution investigations of AK123/FN (Fig. 3E and Fig. S16), we can safely conclude that the developed AK123/FN NCs possess good biosafety profile for potential translation applications.

3. Conclusion

In summary, we developed an advanced nanomedicine formulation based on hydroxyl-terminated bioactive *per se* phosphorus dendrimers complexed with FN for efficient brain delivery to significantly alleviate PD. The developed AK123/FN NCs through physical complexation possess a spherical morphology with a size of 223 nm and good water dispersion stability and cytocompatibility. This unique design not only renders the hydroxyl-terminated phosphoropus dendrimers with water dispersibility but also facilitates the NCs with effective FN-mediated targeting to microglia and hydroxylated dendrimer-enabled BBB crossing ability. The bioactive functions of both dendrimer carriers and FN drug can be exerted to regulate microglia polarization from M1 phenotype to anti-inflammatory M2 one, exert remarkable antioxidant activity to downregulate inflammatory cytokines such as TNF-α, IL-1β, and IL-6, and inhibit NF-κB expression in activated microglia. In a PD mouse model, the AK123/FN NCs are demonstrated to efficiently penetrate the damaged BBB through fluorescence imaging, and exert their anti-inflammatory and antioxidant effects to modulate the brain immune microenvironment, resulting in effective alleviation of the behavioral symptoms of PD mice through gradual restoration of dopamine level, increased expression of TH, as well as decreased expression of IBA-1, GFAP, and α-syn. With the proven good biosafety profile, extended blood circulation time and excellent metabolizability, the developed phosphrous dendrimer/FN NCs not only demonstrate their great potential for the clinical treatment of PD, but also hold great promise to be used to tackle other neurodegenerative disorders.

Ethics approval and consent to participate

All animal experiments were performed in accordance with the guidelines of the Committee on Experimental Animal Care and Use of Donghua University (approval # DHUEC-STCSM-2023-01) and also in accordance with the regulations of the National Ministry of Health of China.

CRediT authorship contribution statement

Waicong Dai: Writing – original draft, Visualization, Validation, Methodology, Investigation, Formal analysis, Data curation. **Mengsi Zhan:** Investigation, Formal analysis, Data curation. **Yue Gao:** Investigation, Data curation. **Huxiao Sun:** Data curation. **Yu Zou:** Data curation. **Régis Laurent:** Data curation. **Serge Mignani:** Supervision, Project administration. **Jean-Pierre Majoral:** Supervision, Resources, Project administration, Funding acquisition. **Mingwu Shen:** Supervision, Resources, Project administration, Funding acquisition. **Xiangyang Shi:** Writing – review & editing, Supervision, Resources, Project administration, Funding acquisition, Conceptualization.

Declaration of competing interest

The authors declare that they have no known competing financial interests or personal relationships that could have appeared to influence the work reported in this paper.

Acknowledgements

This study was financially supported by the National Natural Science Foundation of China (52350710203 and U23A2096), the Science and Technology Commission of Shanghai Municipality (21490711500, 23WZ2503300, 23520712500 and 20DZ2254900), the National Key R&D Program (2022YFE0196900), and the Shanghai Education Commission through the leading talent program. S.M. and X.S. also acknowledge the support by the Fundação para a Ciência e a Tecnologia

(FCT) with Portuguese Government funds through the CQM Base Fund - UIDB/00674/2020 (DOI: 10.54499/UIDB/00674/2020) and Programmatic Fund - UIDP/00674/2020 (DOI: 10.54499/UIDP/00674/2020).

Appendix A. Supplementary data

Supplementary data to this article can be found online at https://doi.org/10.1016/j.bioactmat.2024.04.005.

References

[1] S. Amor, F. Puentes, D. Baker, P. van der Valk, Inflammation in neurodegenerative diseases, Immunology 129 (2) (2010) 154–169.
[2] W. Poewe, K. Seppi, C.M. Tanner, G.M. Halliday, P. Brundin, J. Volkmann, A.-E. Schrag, A.E. Lang, Parkinson disease, Nat. Rev. Dis. Prim. 3 (2017) 17013.
[3] J. Wang, X. Ding, X. Wu, J. Liu, R. Zhou, P. Wei, Q. Zhang, C. Zhang, K. Zen, L. Li, SIRP alpha deficiency accelerates the pathologic process in models of Parkinson disease, Glia 67 (12) (2019) 2343–2359.
[4] W.R.G. Gibb, M.M. Esiri, A.J. Lees, Clinical and pathological features of diffuse cortical lewy body disease (lewy body dementia), Brain 110 (1987) 1131–1153.
[5] L.V. Kalia, A.E. Lang, Parkinson's disease, Lancet 386 (9996) (2015) 896–912.
[6] D.W. Dickson, H. Braak, J.E. Duda, C. Duyckaerts, T. Gasser, G.M. Halliday, J. Hardy, J.B. Leverenz, K. Del Tredici, Z.K. Wszolek, I. Litvan, Neuropathological assessment of Parkinson's disease: refining the diagnostic criteria, Lancet Neurol. 8 (12) (2009) 1150–1157.
[7] B. Yang, Y. Chen, J. Shi, Reactive oxygen species (ROS)-Based nanomedicine, Chem. Rev. 119 (8) (2019) 4881–4985.
[8] Q. Li, B.A. Barres, Microglia and macrophages in brain homeostasis and disease, Nat. Rev. Immunol. 18 (4) (2018) 225–242.
[9] P. Vicente Torres-Ortega, L. Saludas, A.S. Hanafy, E. Garbayo, M. Jose Blanco-Prieto, Micro- and nanotechnology approaches to improve Parkinson's disease therapy, J. Contr. Release 295 (2019) 201–213.
[10] A.M. Palmer, The role of the blood brain barrier in neurodegenerative disorders and their treatment, J. Alzheim. Dis. 24 (4) (2011) 643–656.
[11] N.L. Opie, S.E. John, G.S. Rind, S.M. Ronayne, Y.T. Wong, G. Gerboni, P.E. Yoo, T. H. Lovell, T.C.M. Scordas, S.L. Wilson, A. Dornom, T. Vale, T.J. O'Brien, D. B. Grayden, C.N. May, T. Oxley, Focal stimulation of the sheep motor cortex with a chronically implanted minimally invasive electrode array mounted on an endovascular stent, Nat. Biomed. Eng. 2 (12) (2018) 907–914.
[12] N.J. Abbott, A.A.K. Patabendige, D.E.M. Dolman, S.R. Yusof, D.J. Begley, Structure and function of the blood-brain barrier, Neurobiol. Dis. 37 (1) (2010) 13–25.
[13] T.W. Gardner, D.A. Antonetti, A.J. Barber, E. Lieth, J.A. Tarbell, G. Penn State Retina Res, The molecular structure and function of the inner blood-retinal barrier, Doc. Ophthalmol. 97 (3–4) (1999) 229–237.
[14] A. Patabendige, D. Janigro, The role of the blood-brain barrier during neurological disease and infection, Biochem. Soc. Trans. 51 (2) (2023) 613–626.
[15] S. Liebner, R.M. Dijkhuizen, Y. Reiss, K.H. Plate, D. Agalliu, G. Constantin, Functional morphology of the blood-brain barrier in health and disease, Acta Neuropathol. 135 (3) (2018) 311–336.
[16] W.M. Pardridge, Treatment of Alzheimer's disease and blood-brain barrier drug delivery, Pharmaceuticals 13 (11) (2020) 394.
[17] A.S. Dyatlova, N.S. Novikova, B.G. Yushkov, E.A. Korneva, V.A. Chereshnev, The blood-brain barrier in neuroimmune interactions and pathological processes, herald russ. Acad, Science 92 (5) (2022) 590–599.
[18] A. Sharma, R. Sharma, Z. Zhang, K. Liaw, S.P. Kambhampati, J.E. Porterfield, K. C. Lin, L.B. DeRidder, S. Kannan, R.M. Kannan, Dense hydroxyl polyethylene glycol dendrimer targets activated glia in multiple CNS disorders, Sci. Adv. 6 (4) (2020) eaay8514.
[19] N. Launay, A.M. Caminade, R. Lahana, J.P. Majoral, A general synthetic strategy for neutral phosphorus-containing dendrimers, Angew. Chem., Int. Ed. 33 (15–16) (1994) 1589–1592.
[20] K. Milowska, T. Gabryelak, M. Bryszewska, A.M. Caminade, J.P. Majoral, Phosphorus-containing dendrimers against alpha-synuclein fibril formation, Int. J. Biol. Macromol. 50 (4) (2012) 1138–1143.
[21] K. Milowska, J. Grochowina, N. Katir, A. El Kadib, J.P. Majoral, M. Bryszewska, T. Gabryelak, Viologen-phosphorus dendrimers inhibit α-synuclein fibrillation, Mol. Pharm. 10 (3) (2013) 1131–1137.
[22] W.S. To, K.S. Midwood, Plasma and cellular fibronectin: distinct and independent functions during tissue repair, Fibrogenesis Tissue Repair 4 (1) (2011) 21.
[23] G. Baneyx, L. Baugh, V. Vogel, Fibronectin extension and unfolding within cell matrix fibrils controlled by cytoskeletal tension, Proc. Natl. Acad. Sci. U.S.A. 99 (8) (2002) 5139–5143.
[24] A.R. Pickford, I.D. Campbell, NMR studies of modular protein structures and their interactions, Chem. Rev. 104 (8) (2004) 3557–3565.
[25] D.J. Leahy, I. Aukhil, H.P. Erickson, 2.0 angstrom crystal structure of a four-domain segment of human fibronectin encompassing the RGD loop and synergy region, Cell 84 (1) (1996) 155–164.
[26] H. Liu, Y. Han, T. Wang, H. Zhang, Q. Xu, J. Yuan, Z. Li, Targeting microglia for therapy of Parkinson's disease by using biomimetic ultrasmall nanoparticles, J. Am. Chem. Soc. 142 (52) (2020) 21730–21742.
[27] C.U.A. Kloss, A. Werner, M.A. Klein, J. Shen, K. Menuz, C. Probst, G.W. Kreutzberg, G. Raivich, Integrin family of cell adhesion molecules in the injured brain: regulation and cellular localization in the normal and regenerating mouse facial motor nucleus, J. Comp. Neurol. 411 (1) (1999) 162–178.
[28] L. Guicai, Y. Ping, G. Xiang, H. Nan, S. Ru, An in vitro evaluation of inflammation response of titanium functionalized with heparin/fibronectin complex, Cytokine 56 (2) (2011) 208–217.
[29] X.H. Yuan, Y. Wu, J. Lin, Q.Y. Weng, L.Q. Wu, S. Yang, X. Li, M. Tan, Z.X. Lin, X. L. Lian, Y.Z. Chen, Plasma fibronectin can affect the cytokine profile and monocytes/macrophages function in addition to predicting the prognosis of advanced sepsis, Faseb. J. 36 (3) (2022) e22179.
[30] C.L. Kao, H.T. Lin, Y.W. Chen, Y.C. Chen, F.T. Tsai, Y.L. Chang, S.H. Chiou, D. C. Sheu, H.H. Ku, Fibronectin suppresses lipopolysaccharide-induced liver damage and promotes the cytoprotection abilities of hepatocyte-like cells derived from human bone marrow mesenchymal stem cells, Transplant, SAVE Proc. 39 (10) (2007) 3444–3445.
[31] Z.Y. Qiu, A.H. Kwon, K. Tsuji, Y. Kamiyama, T. Okumura, Y. Hirao, Fibronectin prevents D-galactosamine/lipopolysaccharide-induced lethal hepatic failure in mice, Shock 25 (1) (2006) 80–87.
[32] L. Lv, Y. Xie, K. Li, T. Hu, X. Lu, Y. Cao, X. Zheng, Unveiling the mechanism of surface hydrophilicity-modulated macrophage polarization, Adv. Healthcare Mater. 17 (19) (2018) 1800675.
[33] Y. Gao, W.C. Dai, Z.J. Ouyang, M.W. Shen, X.Y. Shi, Dendrimer-mediated intracellular delivery of fibronectin guides macrophage polarization to alleviate acute lung injury, Biomacromolecules 24 (2) (2023) 886–895.
[34] H.X. Sun, M.S. Zhan, A. Karpus, Y. Zou, J. Li, S. Mignani, J.-P. Majoral, X.Y. Shi, M. Y. Shen, Bioactive phosphorus dendrimers as a universal protein delivery system for enhanced anti-inflammation therapy, ACS Nano 18 (3) (2024) 2195–2209.
[35] A. Karpus, S. Mignani, M. Zablocka, J.P. Majoral, Crown macromolecular derivatives: stepwise design of new types of polyfunctionalized phosphorus dendrimers, J. Org. Chem. 87 (5) (2022) 3433–3441.
[36] J.M. Taylor, B.S. Main, P.J. Crack, Neuroinflammation and oxidative stress: Co-conspirators in the pathology of Parkinson's disease, Neurochem. Int. 62 (5) (2013) 803–819.
[37] E. Lee, J.-C. Eo, C. Lee, J.-W. Yu, Distinct features of brain-resident macrophages: microglia and non-parenchymal brain macrophages, Mol. Cell. 44 (5) (2021) 281–291.
[38] W. Gomes-Leal, Microglial physiopathology: how to explain the dual role of microglia after acute neural disorders? Brain Behav.Neural Regen. Res. 2 (3) (2012) 345–356.
[39] W. Gomes-Leal, Why microglia kill neurons after neural disorders? The friendly fire hypothesis, Neural Regener. Res. 14 (9) (2019) 1499–1502.
[40] J. Li, L. Chen, C.S. Li, Y. Fan, M.S. Zhan, H.X. Sun, S. Mignani, J.-P. Majoral, M. W. Shen, X.Y. Shi, Phosphorus dendron nanomicelles as a platform for combination anti-inflammatory and antioxidative therapy of acute lung injury, Theranostics 12 (7) (2022) 3407–3419.